

Article

The Evaluation of the Crystal Structure and Magnetic Properties of $\text{Eu}_{1.84}\text{Ce}_{0.16}\text{CuO}_{4+\alpha-\delta}$ with Ni Substitution

Muhammad Fadhil Falhan ^{1,*}, Rosaldi Pratama ^{1,2}, Lucia Patia Rochman ¹, Rahma Sundaya Effendi ¹, Yati Maryati ¹, Utami Widayiswari ^{1,3} , Dita Puspita Sari ^{3,4} , Togar Saragi ¹  and Risdiana Risdiana ^{1,*} 

¹ Department of Physics, Padjadjaran University, Jl. Raya Bandung-Sumedang Km. 21, Sumedang 45363, Indonesia; rosaldi17001@mail.unpad.ac.id (R.P.)

² Department of Chemistry, Padjadjaran University, Jl. Raya Bandung-Sumedang Km. 21, Sumedang 45363, Indonesia

³ Meson Science Laboratory, RIKEN Nishina Center, 2-1 Hirosawa, Wako 351-0198, Japan

⁴ Innovative Global Program, College of Engineering, Shibaura Institute of Technology, Saitama City 337-8570, Japan

* Correspondence: muhammad18026@mail.unpad.ac.id (M.F.F.); risdiana@phys.unpad.ac.id (R.R.)

Abstract: The addition of Ni impurities can reveal the correlation between crystal structure changes and magnetic properties and superconductivity. In this study, electron-doped cuprates with an addition of the $\text{Eu}_{1.84}\text{Ce}_{0.16}\text{Cu}_{1-y}\text{Ni}_y\text{O}_{4+\alpha-\delta}$ (ECCNO) Ni impurity, with $y = 0.005, 0.01, 0.02, 0.03,$ and 0.05 in the over-doped regime, was prepared using the solid-state reaction method. The XRD results showed that ECCNO has a T' crystal structure, and lattice parameter c increases when parameters a and b decrease, which causes the distance between the charge reservoir and the conducting layer to become greater, thus affecting magnetic properties. From the superconducting quantum interference device's measurement, it was observed that the magnetic properties of all samples with Ni impurities show a paramagnetic phase, indicating that the effect of Ni impurities could suppress the superconducting phase. It was observed that the Curie constant and the effective magnetic moment tended to decrease for $y \leq 0.02$ and began to increase when $y > 0.02$. This behavior indicated that the effect of the Ni impurity weakened the dynamical Cu spin–spin correlation, which might be related to stripe correlations.

Keywords: Cu spin–spin correlation; effective magnetic moment; electron-doped cuprates; Ni impurity effect



Citation: Falhan, M.F.; Pratama, R.; Rochman, L.P.; Effendi, R.S.; Maryati, Y.; Widayiswari, U.; Sari, D.P.; Saragi, T.; Risdiana, R. The Evaluation of the Crystal Structure and Magnetic Properties of $\text{Eu}_{1.84}\text{Ce}_{0.16}\text{CuO}_{4+\alpha-\delta}$ with Ni Substitution. *Crystals* **2023**, *13*, 1066. <https://doi.org/10.3390/cryst13071066>

Academic Editor: Sergey L. Bud'ko

Received: 12 June 2023

Revised: 1 July 2023

Accepted: 4 July 2023

Published: 6 July 2023



Copyright: © 2023 by the authors. Licensee MDPI, Basel, Switzerland. This article is an open access article distributed under the terms and conditions of the Creative Commons Attribution (CC BY) license (<https://creativecommons.org/licenses/by/4.0/>).

1. Introduction

The potential of high- T_c superconductor cuprates has stood out among all superconductors due to their exotic physical properties and possible applications. All high- T_c superconductor cuprates have the parent compounds of high- T_c cuprates in common, and they are antiferromagnetic (AF). Studies on the mechanism of high- T_c superconductor cuprates have been carried out [1–8]. Nonetheless, these studies have not obtained comprehensive results [9,10]. One way to understand the mechanism of superconductors is to substitute the Cu site with magnetic and non-magnetic impurities in high- T_c superconductor cuprate materials. Hole-doped cuprate studies have been carried out to investigate the intrinsic properties of the material and the effect of impurities on superconductivity [2,3,6,7,11,12]. On the other hand, electron-doped cuprate studies have also succeeded in investigating the effects of magnetic and non-magnetic impurities on superconductivity [4,5]. Superconductor compounds $(\text{Nd, Pr, Sm, and Eu})_{2-x}\text{Ce}_x\text{CuO}_4$ are formed when single-layer CuO_2 materials containing two atoms of rare earth elements, such as Nd, Pr, Sm, or Eu, are doped with Ce^{4+} atoms. Since Eu^{3+} ($4f^6$) does not provide a magnetic moment in its ground state, the effect of impurities on superconductivity can be comprehensively studied [9]. When Eu^{3+} is replaced by Ce^{4+} , an additional electron is added to the CuO_2 plane, leading to the

formation of the $\text{Eu}_{2-x}\text{Ce}_x\text{CuO}_4$ (ECCO) system [1,4,5]. Moreover, due to the difficulty of controlling oxygen concentrations in materials, fewer research studies have been carried out on the impact of impurities on superconductivity in electron-doped cuprates [9,13–15].

The study of the effect of magnetic impurities has caught the attention of researchers interested in evaluating the mechanism of superconductors. Magnetic and non-magnetic impurities can indicate the stripe-pinning model in a hole-doped system. Magnetic and non-magnetic (Ni and Zn) impurity studies on superconductor cuprates showed that these impurities can suppress superconductivity due to weakened Cu spin correlations [1–4,7]. These results are very different compared with iron-based pnictide superconductors, for which their superconductivity is induced by Ni doping [16]. Hole-doped cuprate ($\text{La}_{2-x}\text{Sr}_x\text{CuO}_4$) studies have revealed that magnetic impurities like Ni reduce superconductivity more significantly than non-magnetic impurities like Zn [7]. According to nuclear magnetic resonance measurements, Ni scatters holes weakly, whereas Zn conducts them strongly. It was discovered that as Ni impurity increased, the depolarization data of the muon spin in μSR time spectra showed faster, indicating the development of Cu spin correlations. The decrease in μ_{eff} caused by Ni results in a transition to the under-doped regime, which leads to the formation of Cu spin correlations [7,8,17]. In the CuO_2 planes, Ni has a minor effect on magnetic and electronic states [1].

On the other hand, recent studies on the non-magnetic impurity (Zn) effect on ECCO superconductors showed that Zn suppresses superconductivity and decreases magnetic parameters that could be correlated with stripe-pinning phenomena [4]. Since Eu^{3+} has no magnetic moments, it can be expected that by using ECCO, the effect of Ni impurities on the stripe-pinning model can be observable. Studying the impact of Ni impurities on structural and magnetic properties is necessary as a starting point in order to determine whether the effect of Ni impurities on ECCNO materials can reveal information about the stripe-pinning model. The latest research study reported the presence of magnetic Ni impurities in electron-doped cuprate materials in a heavily under-doped regime with $x = 0.09$ and 0.10 , which showed that Ni could suppress superconductivity with $y = 0.01$ [1]. In other studies of the Ni impurity effect on $\text{Eu}_{2-x}\text{Ce}_x\text{CuO}_4$, possible stripe correlation phenomena at an optimum-doped regime at $x = 0.15$ were observed [17]. However, in the over-doped regime, detailed information on structural and magnetic properties has not been comprehensively studied. When Ni replaces Cu in electron-doped superconducting cuprates, changes in structural and magnetic moments can be implemented as indicators.

To obtain further details, an investigation into the effect of Ni impurities in the over-doped regime with a higher content of y is necessary. We have chosen $x = 0.16$ to strengthen the possibilities of stripe correlations that have been discovered at $x = 0.15$ [17]. Here, we reported the effects of Ni additions of 0.005 , 0.01 , 0.02 , 0.03 , and 0.05 on the magnetic characteristics of the $\text{Eu}_{1.84}\text{Ce}_{0.16}\text{Cu}_{1-y}\text{Ni}_y\text{O}_{4+\alpha-\delta}$ system within the range of an over-doped regime in order to study the structural and magnetic properties of ECCO and the possible existence of stripe correlations in this system.

2. Materials and Methods

All samples of electron-doped cuprate $\text{Eu}_{1.84}\text{Ce}_{0.16}\text{Cu}_{1-y}\text{Ni}_y\text{O}_{4+\alpha-\delta}$ with $y = 0.005$, 0.01 , 0.02 , 0.03 , and 0.05 were synthesized using the solid-state reaction method. The starting precursors were Eu_2O_3 , CeO_2 (Wako Pure Chemical Industries, Ltd., Osaka, Japan, 99.9% purity), NiO (Wako Pure Chemical Industries, Ltd., Osaka, Japan, 99.9% purity), and CuO (Wako Pure Chemical Industries, Ltd., Osaka, Japan, 99.9% purity). All precursors were stoichiometrically combined and pre-fired for 20 h at a temperature of 900°C . The samples were reground and compacted, forming 10 mm diameter pellets before being sintered for 16 h at a temperature of 1000°C . After the second sintering step was completed, as-grown samples were annealed in an argon gas flow at temperatures of 900°C for 10 h to reduce excess oxygen content (α). The reduced oxygen content (δ) with a range from

0.041 to 0.095 [1,4,5] was determined using the mass ratio before and after the annealing process and by using Equation (1):

$$\delta = \left(1 - \frac{m_2}{m_1}\right) \frac{Mr(ECCNO)}{Ar(O)} \quad (1)$$

where m_1 is the mass of the sample before the annealing process, m_2 is the mass of the sample after the annealing process, $Mr(ECCNO)$ is the relative molar mass of $\text{Eu}_{1.84}\text{Ce}_{0.16}\text{Cu}_{1-y}\text{Ni}_y\text{O}_{4+\alpha-\delta}$, and $Ar(O)$ is the relative atomic mass of oxygen.

Energy dispersive X-ray fluorescence (EDXRF) measurements using the ARL Quant'X EDXRF Analyzer on samples with the smallest Ni concentrations were carried out to determine sample composition. X-ray diffractometry (XRD) measurements were carried out at room temperature using PANalytical X'Pert Pro with a Cu-K α radiation source to check the quality of samples and to determine the lattice parameter and bond length. The Rietveld refinement of the XRD patterns was performed in order to analyze the crystal structure, lattice parameters, and bond length. A magnetic properties measurement system (MPMS) with a superconducting quantum interference device (SQUID Quantum Design MPMS XL, San Diego, CA, USA) was used to measure magnetic properties, and these measurements were successfully carried out at different temperatures ranging from 2 K to 30 K in field-cooled (FC) conditions with applied fields at 5 Oe and 500 Oe to study magnetic properties. SQUID measurements were conducted at The Physical and Chemical Research Institute (RIKEN), Wako, Japan.

3. Results and Discussions

Results from EDXRF measurements were used to determine the material's composition. The weight percentage of Eu, Ce, Cu, and Ni exhibits compositions of 61.76%, 5.19%, 17.06%, and 0.058%, respectively. It can be argued that the sample exhibits the correct composition because these results are in close agreement with the results of the composition obtained from calculations, with errors in the calculation of no greater than 15.8%. The XRD results were matched with the used database, which is based on ICSD No. 98-007-1188 [18]. The sample has a tetragonal T' crystal structure ($a = b \neq c$) and planar CuO_2 , which is reflected by the major peaks at Miller indices (013) and (110) with space group of $I4/mmm$ according to the structural parameter analysis from the XRD characterization using the Rietveld refinement shown in Figure 1. All peaks have goodness-of-fit (GoF) range values of 1.403–1.467, which denote a good fit between the data and fitting models. $\text{Eu}_{1.84}\text{Ce}_{0.16}\text{Cu}_{1-y}\text{Ni}_y\text{O}_{4+\alpha-\delta}$ is shown in its crystalline state using various axial views in Figure 2.

Table 1 displays the results of the Rietveld refinement parameters and the bond length. Analyses of lattice parameters a , b , and c showed that when there was an increase in lattice parameters a and b , there was a decrease in lattice parameter c , as shown in Figure 3a. This illustrates the pattern of compensation that occurs between lattices a , b , and c . The changes in lattice parameters a , b , and c when $y < 0.02$ indicated significant changes with respect to the distance between the conducting layer and the charge reservoir of the superconductor, which causes changes in the charge transfer. A similar phenomenon is also observed for the Eu-O bond length; at a concentration of $y = 0.02$, it was observed that when Eu-O(1) bond length decreases, Eu-O(2) bond length increases, as observed in Figure 3b. Thus, there is an increase–decrease compensation pattern between lattices a , b , and c with respect to the Eu-O bond length, particularly at a concentration of $y = 0.02$. Figure 3c,d show that there is no significant change that occurs when the concentration of the Ni impurity is applied to the Cu-O bond length and volume. This could be attributed to the fact that the size of the Ni^{2+} ionic radius is not substantially different from the Cu^{2+} ionic radius.

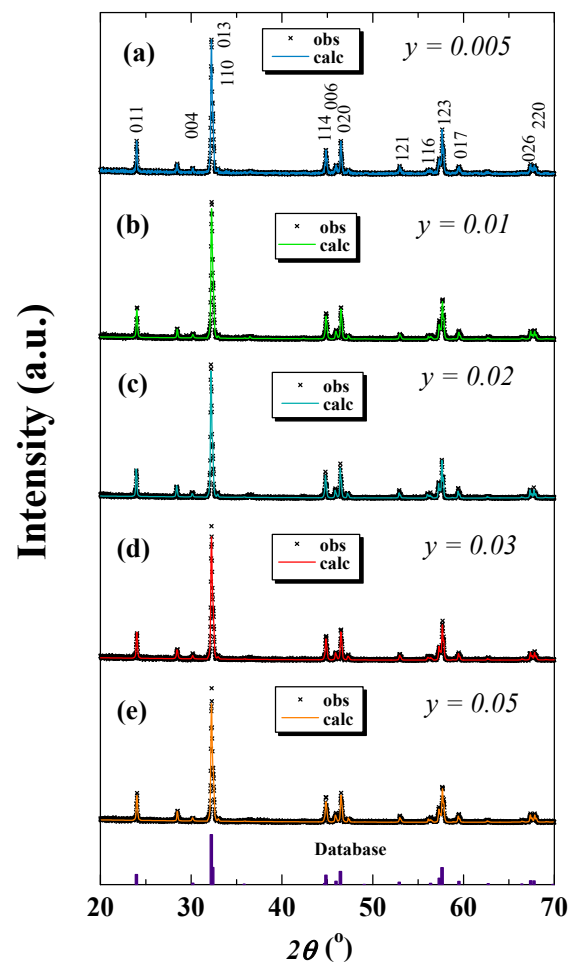


Figure 1. XRD pattern of $\text{Eu}_{1.84}\text{Ce}_{0.16}\text{Cu}_{1-y}\text{Ni}_y\text{O}_{4+\alpha-\delta}$ with $y =$ (a) 0.005, (b) 0.01, (c) 0.02, (d) 0.03, and (e) 0.05.

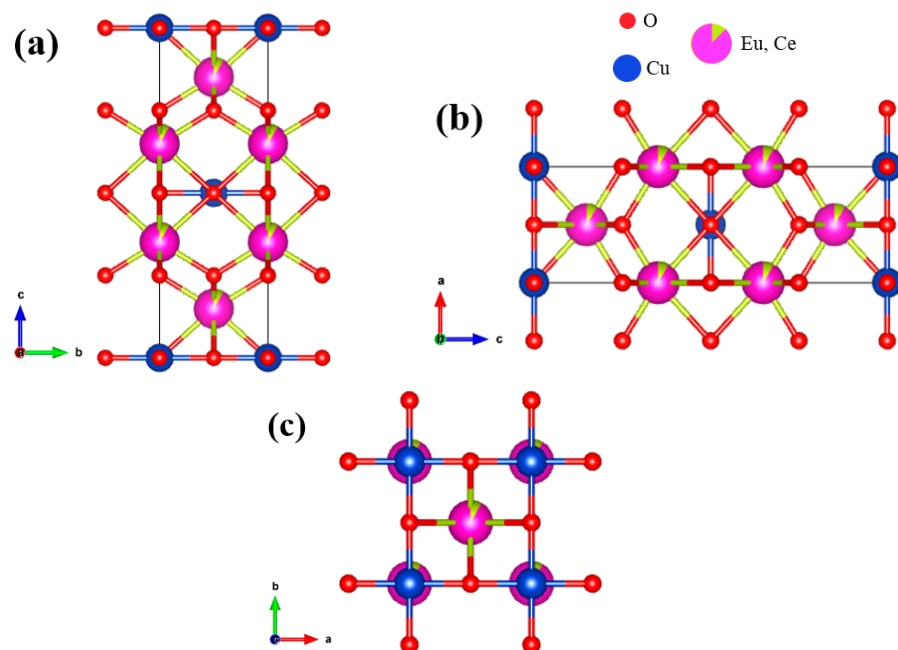


Figure 2. Visualization of the crystal structure from the viewpoint of the (a) a axis, (b) b axis, and (c) c axis.

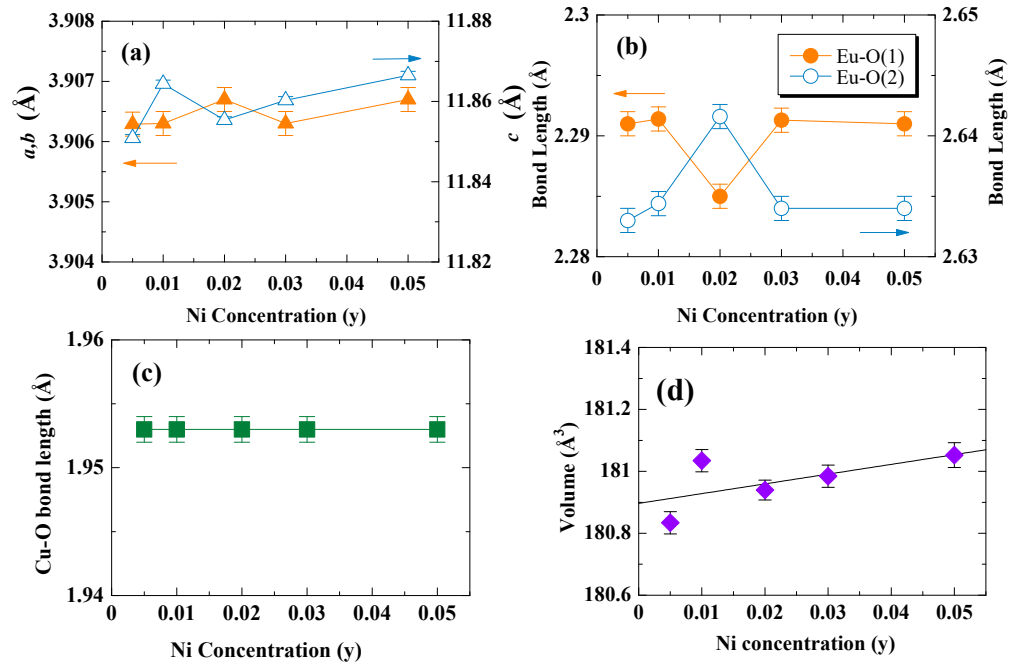


Figure 3. The dependence of Ni concentrations relative to (a) lattice parameters a , b (orange), and c (blue); (b) Eu-O(1) and Eu-O(2) bond-length parameters; (c) Cu-O bond length and (d) volume.

Table 1. Lattice parameters and bond length of $\text{Eu}_{1.84}\text{Ce}_{0.16}\text{Cu}_{1-y}\text{Ni}_y\text{O}_{4+\alpha-\delta}$.

Ce (x)	Ni (y)	Lattice Parameter (\AA)		Volume (\AA^3)	Bond Length (\AA)		
		$a=b$	c		Eu-O(1)	Eu-O(2)	Cu-O
0.16	0.005	3.9063 (2)	11.8508 (9)	180.834 (36)	2.291 (1)	2.633 (1)	1.953 (1)
	0.01	3.9063 (2)	11.8644 (9)	181.034 (36)	2.291 (1)	2.634 (1)	1.953 (1)
	0.02	3.9067 (2)	11.8554 (8)	180.940 (32)	2.285 (1)	2.641 (1)	1.953 (1)
	0.03	3.9063 (2)	11.8603 (9)	180.984 (36)	2.291 (1)	2.634 (1)	1.953 (1)
	0.05	3.9067 (2)	11.8665 (10)	181.052 (40)	2.291 (1)	2.634 (1)	1.953 (1)

In many respects, the development of a magnetic moment as a result of impurity concentrations is a significant topic. It impacts how the CuO_2 layer responds to local changes and how an impurity's electronic state reacts to the CuO_2 environment. The CuO_2 layer's electronic state is disturbed because of the substitution of Ni^{2+} ($3d^8$) ($S = 1, L = 3, J = 4, g_J = \frac{5}{4}$), which has a calculated effective magnetic moment of $5.59 \text{ m}/\mu_B$, at the Cu^{2+} ($3d^9$) ($S = \frac{1}{2}, L = 2, J = \frac{5}{2}, g_J = \frac{6}{5}$) site, which has a calculated effective magnetic moment of $3.54 \text{ m}/\mu_B$. As a result, understanding the role of the CuO_2 layer could be determined by disturbing the CuO_2 environment.

Figure 4 shows the temperature dependence of magnetic susceptibility for $\text{Eu}_{1.84}\text{Ce}_{0.16}\text{Cu}_{1-y}\text{Ni}_y\text{O}_{4+\alpha-\delta}$. For the sample with $y = 0$, the onset critical temperature (T_c) was obtained at a temperature of around 9 K, so it can be said that the pure sample has superconductive characteristics. Meanwhile, samples with Ni impurities show paramagnetic characteristics, as indicated by a positive value of magnetic susceptibility in both given applied fields of 5 Oe and 500 Oe. This indicates that the addition of Ni concentrations of 0.005 can eliminate the superconducting phase of samples. The concentration of Ni impurities on the sample substitutes Cu on the CuO_2 layer, thus eliminating superconductivity.

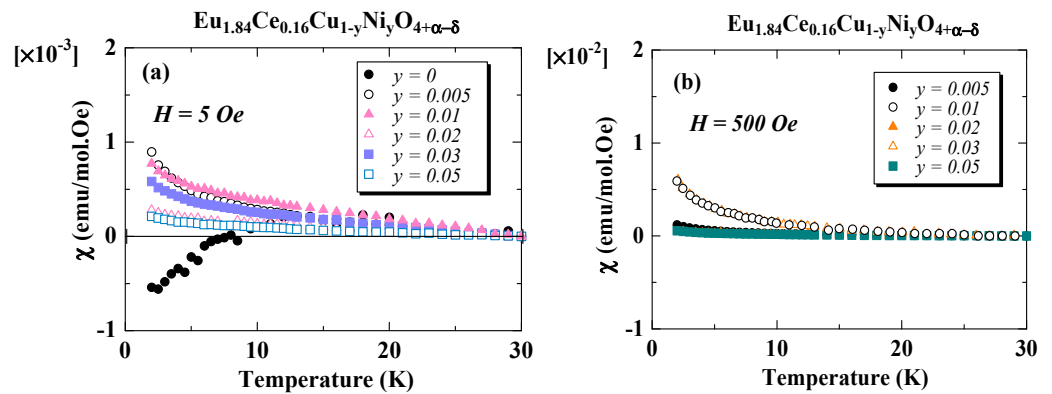


Figure 4. Magnetic susceptibility versus temperatures for $\text{Eu}_{1.84}\text{Ce}_{0.16}\text{Cu}_{1-y}\text{Ni}_y\text{O}_{4+\alpha-\delta}$ with $y = 0, 0.005, 0.01, 0.02, 0.03,$ and 0.05 and (a) $H = 5 \text{ Oe}$ and (b) $H = 500 \text{ Oe}$.

Based on the obtained data, a very small concentration of Ni impurities can eliminate the superconductivity phase. These data also strengthen the results of previous studies [1], thus indicating that the $\text{Eu}_{2-x}\text{Ce}_x\text{CuO}_4$ system has magnetic properties that are sensitive to the addition of Ni magnetic impurities. Compared with another system such as $\text{La}_{2-x}\text{Sr}_x\text{CuO}_4$, the effect of magnetic Ni impurities eliminates superconductivity at $y = 0.05$ [19]. The vanishing superconductivity at $y = 0.005$ in the $\text{Eu}_{2-x}\text{Ce}_x\text{CuO}_4$ system suggests that the substitution of Ni for Cu reduced the magnetization value and the spin–spin correlation in the system, which can lead to the elimination of the superconducting phase.

The Curie constant and effective magnetic moment (μ_{eff}) can be obtained by using

$$\chi = \frac{C}{T} \quad (2)$$

$$\mu_{eff} = \sqrt{3k_B C / N_A \mu_B^2} = 2.828 \sqrt{C} \quad (3)$$

Curie constant C is obtained by using linear regression based on Equation (2) relative to the temperature dependence of the inverse magnetic susceptibility $1/\chi(T)$ curve, where the gradient describes the value of Curie constant C . After the value of the Curie constant is obtained, it can be used to calculate the value of the effective magnetic moment by using Equation (3) in its normal state.

The Curie constant and the effective magnetic moment for all samples are shown in Figure 5a,b, respectively. Curie constant values fall within the range of 5.39–36.49 emu·Oe/mol, and effective magnetic moment values fall within the range of 0.557–1.708 $\mu_B/f.u.$ It was observed that the concentration values tended to decrease until $y < 0.02$ and then tended to increase at $y > 0.02$. At a concentration of $y = 0.02$, there is a minimum value with respect to the Curie constant and the effective magnetic moment. As a result, the pivot point ($y = 0.02$) in the sample illustrates the change from magnetic disorder to magnetic order in the sample. This change in the effective magnetic moment's value is different from the LSCO study with Ni impurities [20], which remained relatively constant at a value of $0.6 \mu_B$, and this is related to the spin state, namely the low-spin state; thus, it could be that the influence of Ni is not only related to the state of the spin but also other phenomena. The value of the sample's effective magnetic moment should increase with the addition of Ni impurities, as observed in the calculated value of the effective magnetic moment where Ni^{2+} is greater than Cu^{2+} . The value of the effective magnetic moment, however, has a tendency to decrease from a range of $y = 0.005$ to 0.02 .

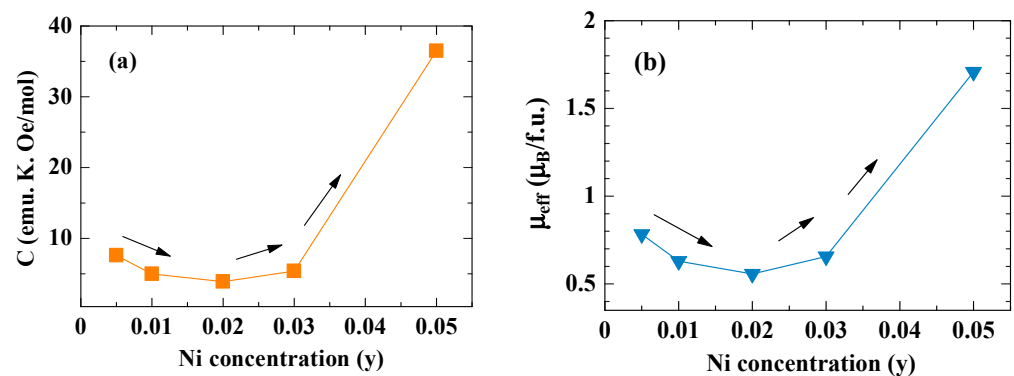


Figure 5. Ni concentration dependencies for the (a) Curie constant and (b) the effective magnetic moment at $H = 500$ Oe.

A decrease in the effective magnetic moment is described as an increase in magnetic disordering in the sample, and an increase in the effective magnetic moment is described as an increase in magnetic ordering in the sample. This indicates that a magnetic order appears when given the Ni concentration reaches a value of $y > 0.02$. The decrease in magnetic properties could be due to the pinning of the dynamical stripe correlation of the spin and charge by Ni^{2+} such that it can weaken the spin–spin correlation of Cu atoms and suppress superconductivity [17]. This number is consistent with the investigation of the effects of Ni on ECCO using μSR measurements, where at concentrations of $y < 0.02$, muon-spin depolarization quickens, which shows a significant weakening of the Cu-spin fluctuation [8,17]. The increase in magnetic properties can be indicated by the fact that the limit value for Ni concentrations to weaken the spin correlation of Cu atoms for $\text{Eu}_{2-x}\text{Ce}_x\text{CuO}_4$ cuprates is $y = 0.02$. When $y > 0.02$, the limit value restores the initial properties of Ni, which then becomes a magnetic impurity that can add to the magnetic value, thus increasing the value of the magnetic parameters in the material. Therefore, based on the changes in the value of the effective magnetic moment by Ni magnetic impurities, in the over-doped region of the $\text{Eu}_{2-x}\text{Ce}_x\text{CuO}_4$ material, there is an indication of the stripe phenomenon, thus strengthening the possibility of the existence of the stripe model in electron-doped cuprates. Further research using advanced measurement techniques (for example, μSR measurements) is necessary to confirm stripe-pinning phenomena in electron-doped cuprates.

4. Conclusions

The electron-doped cuprates of $\text{Eu}_{1.84}\text{Ce}_{0.16}\text{Cu}_{1-y}\text{Ni}_y\text{O}_{4+\alpha-\delta}$ with $y = 0.005, 0.01, 0.02, 0.03,$ and 0.05 were successfully synthesized to investigate the effect of Ni impurities on the magnetic properties of over-doped regimes in electron-doped systems. Based on XRD measurements, it was observed that lattice parameter c increases when parameters a and b decrease and vice versa, which causes the distance between the charge reservoir and the conducting layer to become greater. Accordingly, superconductivity does not appear due to the charge carrier transfer difficulty. Based on the SQUID measurement, all samples with Ni impurities have paramagnetic characteristics indicated by a positive magnetic susceptibility value. Superconductivity vanished in all samples, suggesting that the addition of Ni impurities could eliminate the superconducting phase in $\text{Eu}_{2-x}\text{Ce}_x\text{CuO}_4$ cuprates. There is a transition between magnetic disorder and magnetic order properties at a pivot point of $y = 0.02$. The behavior of decreasing magnetic parameters could be correlated with the dynamical stripe correlation, which results in stripe-pinning phenomena, strengthening the possibility of the stripe model in electron-doped cuprates. Further research is necessary to confirm stripe-pinning phenomena in electron-doped cuprates.

Author Contributions: Conceptualization, M.F.F., T.S. and R.R.; methodology, M.F.F., R.P., L.P.R., R.S.E., Y.M., U.W., D.P.S., T.S. and R.R.; software, M.F.F. and R.P.; formal analysis, M.F.F., R.P., L.P.R., R.S.E., Y.M., U.W., D.P.S. and R.R.; investigation, M.F.F., R.P. and U.W.; resources, M.F.F. and L.P.R.; data curation, T.S. and R.R.; writing—original draft preparation, M.F.F.; writing—review and editing, T.S. and R.R.; visualization, M.F.F.; supervision, T.S. and R.R.; project administration, R.R.; funding acquisition, R.R. All authors have read and agreed to the published version of the manuscript.

Funding: This work was supported by Kemenristek-DIKTI of Indonesia with respect to financial support for this research study within the scheme of the Thesis Magister Grant (PTM) 2022, Contract No. 1318/UN6.3.1/PT.00/2022, and it is also partially supported by the Academic Leadership Grant of Universitas Padjadjaran 2022, No. 2203/UN6.3.1/PT.00/2022.

Data Availability Statement: Not applicable.

Acknowledgments: We would like to thank Isao Watanabe and all members of The Physical and Chemical Research Institute (RIKEN, Wako, Japan) for providing SQUID measurements and hosting the Sakura Program. These works were supported by the Japan Science and Technology Agency.

Conflicts of Interest: The authors declare no conflict of interest.

References

- Rochman, L.P.; Anggia, H.D.; Pratama, R.; Maulana, T.; Winarsih, S.; Maryati, Y.; Syakuur, M.A.; Widyaiswari, U.; Sari, D.P.; Saragi, T.; et al. Effect of Additional Magnetic Material Ni on Structure and Magnetic Properties $\text{Eu}_{2-x}\text{Ce}_x\text{Cu}_{0.99}\text{Ni}_{0.01}\text{O}_{4+\alpha-\delta}$. *J. Phys. Conf. Ser.* **2022**, *2165*, 012020. [\[CrossRef\]](#)
- Matsuda, M.; Fujita, M.; Yamada, K. Impurity Effect on the Diagonal Incommensurate Spin Correlations in $\text{La}_{2-x}\text{Sr}_x\text{CuO}_4$. *Phys. Rev. B* **2006**, *73*, 140503. [\[CrossRef\]](#)
- Suzuki, K.; Adachi, T.; Tanabe, Y.; Koike, Y.; Kawamata, T.; Risdiana; Suzuki, T.; Watanabe, I. Hole Trapping by Ni, Kondo Effect, and Electronic Phase Diagram in Nonsuperconducting Ni-Substituted $\text{La}_{2-x}\text{Sr}_x\text{Cu}_{1-y}\text{Ni}_y\text{O}_4$. *Phys. Rev. B* **2010**, *82*, 054519. [\[CrossRef\]](#)
- Pratama, R.; Saragi, T.; Maulana, T.; Winarsih, S.; Maryati, Y.; Syakuur, M.A.; Widyaiswari, U.; Sari, D.P.; Manawan, M.; Risdiana, R. Changes in the Structural Parameters and Effective Magnetic Moment of $\text{Eu}_{2-x}\text{Ce}_x\text{CuO}_{4+\alpha-\delta}$ by Zn Substitution. *Coatings* **2022**, *12*, 789. [\[CrossRef\]](#)
- Syakuur, M.A.; Pratama, R.; Anggia, H.D.; Rochman, L.P.; Maryati, Y.; Saragi, T.; Risdiana. Enhanced Magnetic Ordering by Impurity Fe Substitution on Electron-Doped Superconductors $\text{Eu}_{2-x+y}\text{Ce}_{x-y}\text{Cu}_{1-y}\text{Fe}_y\text{O}_{4+\alpha-\delta}$. *Heliyon* **2022**, *8*, e11501. [\[CrossRef\]](#) [\[PubMed\]](#)
- Shakeripour, H.; Hosseini, S.S.; Ghotb, S.S.; Hadi-Sichani, B.; Pourasad, S. Magnetic Doping Effects on the Superconductivity of $\text{Y}_{1-x}\text{M}_x\text{Ba}_2\text{Cu}_3\text{O}_{7-\delta}$ (M = Fe, Co, Ni). *Ceram. Int.* **2021**, *47*, 10635–10642. [\[CrossRef\]](#)
- Adachi, T.; Yairi, S.; Koike, Y.; Watanabe, I.; Nagamine, K. Muon-Spin-Relaxation and Magnetic-Susceptibility Studies of the Effects of the Magnetic Impurity Ni on the Cu-Spin Dynamics and Superconductivity in $\text{La}_{2-x}\text{Sr}_x\text{Cu}_{1-y}\text{Ni}_y\text{O}_4$ with $x = 0.13$. *Phys. Rev. B* **2004**, *70*, 060504. [\[CrossRef\]](#)
- Tranquada, J.M.; Sternlieb, B.J.; Axe, J.D.; Nakamura, Y.; Uchida, S. Evidence for Stripe Correlations of Spins and Holes in Copper Oxide Superconductors. *Nature* **1995**, *375*, 561–563. [\[CrossRef\]](#)
- Armitage, N.P.; Fournier, P.; Greene, R.L. Progress and Perspectives on Electron-Doped Cuprates. *Rev. Mod. Phys.* **2010**, *82*, 2421–2487. [\[CrossRef\]](#)
- Niedermayer, C.; Bernhard, C.; Blasius, T.; Golnik, A.; Moodenbaugh, A.; Budnick, J.I. Common Phase Diagram for Antiferromagnetism in $\text{La}_{2-x}\text{Sr}_x\text{CuO}_4$ and $\text{Y}_{1-x}\text{Ca}_x\text{Ba}_2\text{Cu}_3\text{O}_6$ as Seen by Muon Spin Rotation. *Phys. Rev. Lett.* **1998**, *80*, 3843–3846. [\[CrossRef\]](#)
- Tanabe, Y.; Adachi, T.; Noji, T.; Koike, Y. Superconducting Volume Fraction in Overdoped Regime of $\text{La}_{2-x}\text{Sr}_x\text{CuO}_4$: Implication for Phase Separation from Magnetic-Susceptibility Measurement. *J. Phys. Soc. Jpn.* **2005**, *74*, 2893–2896. [\[CrossRef\]](#)
- Panagopoulos, C.; Petrovic, A.P.; Hillier, A.D.; Tallon, J.L.; Scott, C.A.; Rainford, B.D. Exposing the Spin-Glass Ground State of the Nonsuperconducting $\text{La}_{2-z}\text{Sr}_x\text{Cu}_{1-y}\text{Zn}_y\text{O}_4$ High-Tc Oxide. *Phys. Rev. B* **2004**, *69*, 144510. [\[CrossRef\]](#)
- Adachi, T.; Mori, Y.; Takahashi, A.; Kato, M.; Nishizaki, T.; Sasaki, T.; Kobayashi, N.; Koike, Y. Evolution of the Electronic State through the Reduction Annealing in Electron-Doped $\text{Pr}_{1.3-x}\text{La}_{0.7}\text{Ce}_x\text{CuO}_{4+\delta}$ ($x = 0.10$) Single Crystals: Antiferromagnetism, Kondo Effect, and Superconductivity. *J. Phys. Soc. Jpn.* **2013**, *82*, 063713. [\[CrossRef\]](#)
- Sumura, T.; Ishimoto, T.; Kuwahara, H.; Kurashima, K.; Koike, Y.; Watanabe, I.; Miyazaki, M.; Koda, A.; Kadono, R.; Adachi, T. Reduction Effects on the Cu-Spin Correlation in the Electron-Doped T'-Cuprate $\text{Pr}_{1.3-x}\text{La}_{0.7}\text{Ce}_x\text{CuO}_{4+\delta}$ ($x = 0.10$). *JPS Conf. Proc.* **2018**, *21*, 011027. [\[CrossRef\]](#)
- Higgins, J.S.; Dagan, Y.; Barr, M.C.; Weaver, B.D.; Greene, R.L. Role of Oxygen in the Electron-Doped Superconducting Cuprates. *Phys. Rev. B* **2006**, *73*, 104510. [\[CrossRef\]](#)
- Li, Y.K.; Lin, X.; Zhou, T.; Shen, J.Q.; Tao, Q.; Cao, G.H.; Xu, Z.A. Superconductivity Induced by Ni Doping in $\text{SmFe}_{1-x}\text{Ni}_x\text{AsO}$. *J. Phys. Condens. Matter* **2009**, *21*, 355702. [\[CrossRef\]](#)

17. Risdiana, R.; Safriani, L.; Somantri, W.A.; Saragi, T.; Adachi, T.; Kawasaki, I.; Watanabe, I.; Koike, Y. Possible Existence of the Stripe Correlations in Electron-Doped Superconducting Cuprates $\text{Eu}_{1.85}\text{Ce}_{0.15}\text{Cu}_{1-y}\text{Ni}_y\text{O}_{4+\alpha-\delta}$ Studied by Muon-Spin-Relaxation. In *Advanced Materials Science and Technology*; Advanced Materials Research; Trans Tech Publications Ltd.: Stafa-Zurich, Switzerland, 2014; Volume 896, pp. 354–357. [[CrossRef](#)]
18. Uzunaki, T.; Kamehara, N.K.N.; Niwa, K.N.K. Crystal Structure and Madelung Potential in $\text{R}_{2-x}\text{Ce}_x\text{CuO}_{4-\delta}$ (R = Pr, Nd, Sm, Eu and Gd) System. *Jpn. J. Appl. Phys.* **1991**, *30*, L981. [[CrossRef](#)]
19. Adachi, T.; Oki, N.; Risdiana; Yairi, S.; Koike, Y.; Watanabe, I. Relationship between the Cu-Spin Fluctuation and Superconductivity in $\text{La}_{2-x}\text{Sr}_x\text{Cu}_{1-y}(\text{Zn},\text{Ni})_y\text{O}_4$ ($x = 0.15$) Studied by the MSR and Magnetic-Susceptibility. *Phys. C Supercond.* **2007**, *460–462*, 1172–1173. [[CrossRef](#)]
20. Xiao, G.; Cieplak, M.Z.; Xiao, J.Q.; Chien, C.L. Magnetic Pair-Breaking Effects: Moment Formation and Critical Doping Level in Superconducting $\text{La}_{1.85}\text{Sr}_{0.15}\text{Cu}_{1-x}\text{A}_x\text{O}_4$ Systems (A = Fe, Co, Ni, Zn, Ga, Al). *Phys. Rev. B* **1990**, *42*, 8752–8755. [[CrossRef](#)]

Disclaimer/Publisher’s Note: The statements, opinions and data contained in all publications are solely those of the individual author(s) and contributor(s) and not of MDPI and/or the editor(s). MDPI and/or the editor(s) disclaim responsibility for any injury to people or property resulting from any ideas, methods, instructions or products referred to in the content.